



# Effect of LEO (*Lycium* Essential Oils) as Green Inhibitors of Calcium Carbonate Scale on Nanoparticles-Doped Ultrafiltration Membrane (UFM) and Water Treatment

Zahrah Alhalili<sup>1</sup> · Hana Souli<sup>2</sup> · Moêz Smiri<sup>1,2</sup>

Received: 6 January 2021 / Accepted: 8 September 2021  
© King Fahd University of Petroleum & Minerals 2021

## Abstract

Considering the growing environmental concerns about the discharge of saline water coming from desalination systems, the present work is of significant interest. The effect of LEO (*Lycium* Essential Oils) as green inhibitors of calcium carbonate scale has been investigated in this study. We used conductivity measurements, nanoparticles-doped membranes technologies, electrochemical impedance spectroscopy (EIS), and chronoamperometry techniques. The calcium carbonate scale was deposited from the brine solution by cathodic polarization of the steel surface. The observed anti-scaling property can be partly explained by the presence of plant antioxidants. Antioxidants retarded calcium carbonate precipitation via the formation of a complex with the calcium cations. Without LEO, adherent film formed over the steel surface, under cathodic polarization, by the deposition of the calcium complex.

**Keywords** Anti-scalant · Chronoamperometry · Electrochemical Impedance Spectroscopy (EIS) · Extract · Inhibitors · *Lycium* Essential Oils (LEO) · Nanoparticles (NPs) · Scales · Ultrafiltration Membranes (UFM)

## Abbreviations

CaCO <sub>3</sub>	Calcium carbonate
EIS	Electrochemical Impedance Spectroscopy
LEO	<i>Lycium</i> Essential oil
MUF	Ultrafiltration membrane
NPs	Nanoparticles
R <sub>p</sub>	Polarization resistance
SCE	Saturated calomel electrode

## 1 Introduction

The genus *Lycium* appeared 29.4 million years ago in the New World, and then spread to Southern Africa and from there to Eurasia and Australia. This genus of species is dispersed in temperate and subtropical regions [1]. In North and South America, 20 and 30 species were identified,

respectively, whereas 20 species were listed in Southern Africa. The number of species found in Eurasia (from Europe to China and Japan) was 10, and there are only two and one in the Pacific Islands and Australia, respectively. According to the phylogenetic classification [2], Goji belongs to the Angiosperms evolved dicotyledons, named Asteroids. It belongs to the order Solanales, the family Solanaceae and the genus *Lycium*, small trees with a height varying from 80 to 3 m (Fig. 1). Most of them grow in arid or subarid regions, whereas a few are in coastal areas on saline soils [1]. They were known in traditional medicine and served as functional foods [2]. The leaves were deciduous, thick, solitary, or fasciculate and lanceolate or long elliptic, 2 to 3 cm long and 36 mm wide and of a green color bright enough for the young and then changed to gray. They contain various compounds such as flavonoids (such as ketin, kaempferol, rutin, nicotiflorin, and isoquercitrin) as well as other molecules like vanillic acid, salicylic acid, and nicotinic acid [3]. The purple-colored flowers were carried by a pedicel with the campanulate calyx of 4 to 5 mm and the bloom was spread out from June to September. The fruits of common and Chinese *Lycium* were the most used species in oriental medicine called Tibeticum due to the shrub producing berries called Goji berries, which was a red berry (more

✉ Moêz Smiri  
almoez@su.edu.sa; smirimoez@yahoo.fr

<sup>1</sup> Shaqra University, College of Sciences and Arts–Sajir, Riyadh, Saudi Arabia

<sup>2</sup> ISSTE, Carthage University, Technopole of Borj Cedria, 2050 Hammam-Lif, Tunisia



**Fig. 1** Photograph from *Lycium Barbarum*



or less orange), turning the sweet flavor into somewhat bitter. They ripened from August to October [3–6].

Scaling has been known by the formation of stalactites and stalagmites, which essentially comprised calcium carbonate ( $\text{CaCO}_3$ ), whose formation process is inseparable from the carbon dioxide ( $\text{CO}_2$ ) degassing of natural water [7]. The adherent crystalline deposit was mainly formed of calcium carbonate  $\text{CaCO}_3$  [8] and magnesium hydroxide  $\text{Mg}(\text{OH})_2$ , which is formed from a heating temperature above  $50\text{ }^\circ\text{C}$  [9]. The precipitation of mineral scales on heat transfer surfaces widely occurs in numerous industrial processes. Deposits formation may cause severe corrosion and deteriorate conditions of the heat exchange [10]. These deposits were generally observed in domestic and industrial installations distribution water circuits, especially in membrane desalination operations with high recovery rates, petroleum production equipment surfaces, cooling water systems, boilers, secondary oil recovery, and desalination

plants [11]. Among the main problems encountered in water desalination was scale formation, which caused major economic problems in both industry and domestic installations. This results in flow decline, reduced process efficiency, and increased operating costs. It also limits heat exchange and reduces tube diameter [12]. Inorganic scale formation in the wellbore, surface facilities, and near-wellbore formation is a common cause of production loss in most matured fields. The precipitation of  $\text{CaCO}_3$  and the formation of compact and adherent scale deposits on the surface of pipes and domestic or industrial structures have serious technical and economic consequences: clogging of pipes, and invasion by the scale of hot water production systems (boilers, heat exchangers, ... etc.), reduction in the heat transfer coefficient, reduction in the diameter of water pipes, etc.

Owing to its inverse temperature-solubility characteristics,  $\text{CaCO}_3$  was the predominant component of scales deposited from natural water, especially in cooling water



systems [13]. Unless treated, the scale formed on the surface continued to get thicker [14]. Calcium concentration and supersaturation, water hardness, temperature, water composition, pH, CO<sub>2</sub>, pressure or/and nature of the substrate in contact with water influence scale formation [14]. Many scale inhibitors have been used in cooling water systems [15], such as the chemical anti-scaling process: the use of chemical inhibitors, acid, lime decarbonation, demineralization on ion exchange resins, the physical process: the micro-electrolysis of water, the generation of high-frequency electromagnetic waves sent in antennas wound on pipes, and the passage of water through permanent magnets. Many products prevented scale, organic substances, polyacrylic acid, polyacrylamide, phosphonates, and copolymers [16, 17]. Studies have shown that plant extracts can be used as naturally synthesized inhibitors of scaling with low cost [11]. Green Chemistry products were proposed as ecological and environmental scale inhibitors and became a focus of water treatment technology [16]. Extracts from some plant species through the word were employed as scale inhibitors. Many new cleaning chemicals are synthesized via plants. *Lycium* (*Lycium barbarum* L.) (Fig. 1) is one of the important trees in the Mediterranean coastal zone, which grows well under calcareous soil conditions, and is employed as an incredible source of chemical compounds, especially essential oils (Table 1) [10, 18–20].

An essential oil (EO) contains mainly volatile terpenes, resulting from the condensation of isoprene units and aromatic derivatives of phenylpropane [21]. The Terpenoids were a group of natural products of diverse structures. They are considered the most volatile terpene compounds (hydrocarbons) of the general gross formula (C<sub>5</sub>H<sub>8</sub>)<sub>n</sub> (with  $n = 1$  isoprene). The monoterpenes were one of the main elements of aromatic plant essences called essential oils, they have ten carbon atoms and have two isoprene units, and they can be acyclic, monocyclic, bicyclic, and

tricyclic. Sesquiterpenes belonged to the same chemical families found in monoterpenes but they differ by their skeleton, which contained 15 atoms and three isoprene units (Fig. 2). The present study aimed to investigate LEO as a new environmentally friendly anti-scalant. We used electrochemical impedance spectroscopy (EIS), chrono-amperometry techniques, conductivity measurements, and Ultrafiltration Membranes (UFM) to analyze CaCO<sub>3</sub> calcareous deposits on steel in an alkaline CaCl<sub>2</sub> brine solution.

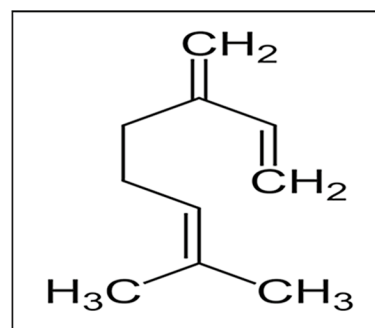
## 2 Materials and Methods

### 2.1 Geographical Location of the Study Area

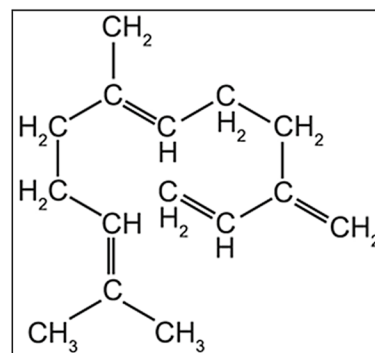
The sample used was from *Lycium* (*Lycium barbarum* L.) which comes from Borj Cedria south-east of Tunisia whose geographical parameters were 36° 44' Latitude and 10° 21' Longitude (Fig. 3). The climatic zone was moderate and semi-arid.

**Table 1** Goji berry compositions [10, 13, 25–27]

Compounds	Specificities
Protein	6–16%
Carbohydrates	40–60% of which 31% specific polysaccharides
Lipids	0.45–1.40%
Fibers	21%
Essential fatty acids	Oil linoleic acid mainly
Amino acids (AA)	19 AA Including the 8 essential amino acids
Vitamins	B1, B2, B3 and C
Minerals	Calcium, magnesium, potassium, phosphorus
Trace elements	Iron, Selenium, Copper, Zinc
Polyphenols	0.003–0.5% (xanthophylls)
Bioactive Substances	p-Coumaric acid, betaine, cerebroside



**Monoterpene**



**Sesquiterpene**

**Fig. 2** Main elements of aromatic plant essences called essential oils



**Fig. 3** Geographical location of the study area



## 2.2 Plant Harvest and Conservation

Leaves of *Lycium* were freshly harvested and dried in open air for 15 days. Once they were dried, they were kept in clean bags to be used later for the extraction of essential oil.

## 2.3 Extraction of Essential Oil

As previously described, reflux assembly was used to extract essential oils [22]. It consisted of a heater flask comported leaves and solvents. By adopting a refrigerant above the heating system, the vapors condensed and fall back into the flask. One hundred gram of dried leaves was placed in a 2500-mL round flask with 440 mL cyclohexane. The mixture is brought to a temperature of 80 °C for 5 h 30 mn. The essential oil was entrained by the solvent vapor before being condensed through the condenser and filled back into the flask. The liquid was

sucked out with a water tube or pump according to vacuum filtration or Büchner filtration. The distillate recovered from the filtration process was placed in a rotary evaporator flask in a water bath with a temperature of 49 °C for 3 h.

## 2.4 Purification

Purification of the recovered sample was carried out by a column comprising at the bottom 2 g of sodium sulfate and at the top 1 g of silica gel which has been activated by a temperature of 40 °C in the oven. Then, our sample was added to the column and dosed with cyclohexane. Thereafter, the LEO recovered from the purification was dried by nitrogen for 15 min under a pressure of 2 bar. Once the essential oils were obtained, we keep them at a temperature of around 4 °C in opaque bottles hermetically sealed to protect them from air and light.

## 2.5 Determination of LEO Rate

The essential oil yield was defined as the ratio between the mass of essential oil obtained and the plant mass to be treated [23].

$$\text{REO (\%)} = \text{MEO/MS} \times 100.$$

REO (%): Essential oil yield.

MEO: Quantity of extract of oil recovered expressed in g (gram of essential oil).

MS: Quantity of dried plant material used for extraction expressed in g (100 g of dry matter).

## 2.6 Determination of Density of LEO

It was defined as the ratio between the mass of LEO obtained and the mass of the same volume of water.

Density = (Mass volume of essential oil)/(Mass of the same volume of water).

## 2.7 Membrane Technology Study

In this study, membrane-based polymer polysulfone, with a circular geometry and surface area of 28.26 cm<sup>2</sup> were used. Fe<sub>2</sub>O<sub>3</sub> iron oxide nanoparticles with a size of 15 ± 2 nm were mixed with polysulfone (PSF) in the 0.5% wt lower load to prepare the UF membrane (UFM) using the wet phase inversion method. Membranes were characterized with X-ray crystallography, whereas the UFM performance was examined by measuring permeate flow and rejection [24]. The permeate flux was evaluated by the equation:

$$J = V/S * T$$

*J*: Permeate flow in (L/m<sup>2</sup>h).

*V*: Volume of accumulated permeate (L) *T*: Filtration time (h).

*S*: Surface area of membrane manufactured (m<sup>2</sup>).

We analyzed the capacity of UFM by frontal filtration. The supply tank and the front filter cell containing the circular membrane coupon are filled with the solution to be filtered, after which the air is removed from the system through a valve located on the lid of the filter cell. The nitrogen bottle provided the operating pressure, which, in turn, was regulated by a pressure relief valve located on the bottle. The pressure was read on the manometer. The permeate exited the cell, while the solution was concentrated in the cell and then filtered. The membrane was compacted with 50 mL of distilled water for 30 min at 5 bars (Table 2). This technique was undertaken to open the pores of the membrane and to allow it to attach better to UFM. Then, 100 mL of an aqueous solution of CaCl<sub>2</sub> 0.7 M was prepared. The solution was characterized by an acid pH of 5.81 and a very high

**Table 2** Table of diaphragm performance as a function of pressure

P (bar)	2	3	4	5
<i>S</i> (m <sup>2</sup> )	0.002826	0.002826	0.002826	0.002826
<i>V</i> (L)	0.003	0.003	0.003	0.003
<i>T</i> (h)	0.065277	0.043888	0.034444	0.026666
<i>J</i> (L/m <sup>2</sup> h)	16.26255	24.18818	30.82020	39.80991

conductivity of 97 ms/cm. For the siltation experiment, only 50 mL of CaCl<sub>2</sub> was versed into the supply tank, after which we started the motor and opened the bottle of nitrogen at 4 bars for 1 h. Following the siltation performed in the first experiment, the membrane was thoroughly washed with distilled water. In the second experiment, LEO was placed on the surface of the membrane and then, the remaining 50 mL of CaCl<sub>2</sub> was versed. This experiment was carried out under the same conditions. The conductivity test setup was as described elsewhere [11]. Measurements were done at 25 °C.

## 2.8 Electrochemical Study

Materials: NaCl, NaHCO<sub>3</sub>, Na<sub>2</sub>SO<sub>4</sub>, and CaCl<sub>2</sub> of analytical reagent grade, were used for preparing solutions with double distilled water. CaCl<sub>2</sub> brine solution was prepared to a concentration of 0.7 M NaCl, 0.0025 M NaHCO<sub>3</sub>, 0.028 M Na<sub>2</sub>SO<sub>4</sub> and 0.01 M CaCl<sub>2</sub>.

The electrochemical measurements were carried out in a cell with three-electrode mode; platinum sheet and saturated calomel electrode (SCE) were used as counter and reference electrodes. Imposed potential chronoamperometry comprised accelerated precipitation of calcium carbonate of electrode raised to an adequate potential to reduce dissolved oxygen in order to produce hydroxyl ions, thus increasing the interfacial pH necessary for calcium deposition [11]. This potential was determined from the polarization curve (voltammetry curve ( $I=f(E)$ )) of the working electrode immersed in the water to be analyzed in accordance with the method proposed by Lédion et al. [25]. Autolab potentiostat driven by the Nova 1.7 software allowed us to record the polarization curves  $I=f(E)$  and the chronoamperometric curves along with the electrochemical impedance spectra with the help of an experimental device. This software allowed data processing and the establishment of relationships between potential, current, and time to determine the various electrochemical parameters. The different electrodes used in chronoamperometry were (1) reference electrode (it was impolarizable; its potential was rigorously constant; it was measured in relation to the hydrogen electrode, (2) auxiliary electrode (counter electrode, it was made of platinum reference "Wire" type B35M110 and was placed in front of the working electrode to ensure the passage of the current



and (3) working electrode. With regard to our experiments, we used a 500 mL stock solution of  $\text{CaCl}_2$ ,  $\text{NaCl}$ ,  $\text{Na}_2\text{SO}_4$ ,  $\text{NaHCO}_3$  as electrolyte for the electrochemical tests, with concentrations of 0.01 M  $\text{CaCl}_2$ , 0.7 M  $\text{NaCl}$ , 0.028 M  $\text{Na}_2\text{SO}_4$ , and 0.0025 M  $\text{NaHCO}_3$ , respectively. Table 3 shows the characteristics of the electrolyte solution. We prepared two solutions; the first one was a control solution (250 mL without LEO) and the second one was a treated solution (250 mL with LEO; we take 4 mL and replace them with 4 mL of LEO).

## 2.9 Chronoamperometric Experiments

As described previously, experiments were carried out in a cylindrical electrochemical cell made of "PYREX" glass with a volume of 250 mL, equipped with a three-electrode assembly [11]. These different electrodes were used to study the scaling of the solution as well as the scaling effect of the LEO: reference electrode, auxiliary electrode, and working electrode, which was a glass substrate with an insulating layer and a conductive layer which was FTO (Fluorine Tin Oxide) layer. This layer was placed opposite to the counter electrode (this was the layer on which  $\text{CaCl}_2$  was deposited). The first chronoamperometry analysis was performed on the control solution without LEO at a temperature of 40 °C under magnetic agitation and we imposed a potential of  $-0.9$  V during 2 h. The follow-up of the current evolution as a function of time allowed us to obtain a chronoamperometry curve. The second experiment was carried out on the solution with LEO whose conditions were the same: we followed the current for 2 h to have the chronoamperometry curve which will allow us to have the effect of the LEO on the anti-scaling.

### 2.9.1 Electrochemical Impedance Spectroscopy (EIS)

It consisted in measuring the current response of the electrochemical system to potential perturbation by the sinusoidal signal of low amplitude around the stationary value of polarization [11]. The current response is also sinusoidal, superimposed on a stationary current, but out of phase by an angle  $\alpha$  with reference to the potential. It brings into play a large frequency domain, which will allow the differentiation of various elementary phenomena according to

their time constants. The fast phenomena will be solicited by high frequencies (case of load transfers) and the slow phenomena will appear with low frequencies (case of matter transport). In the potentiostatic mode, a sinusoidal voltage  $\Delta E(t)$  is superimposed on a DC voltage of bias  $E_0$ .

The potential  $E(t)$  imposed on the system is written:  $E(t) = E_0 + \Delta E(t)$ .

With  $\Delta E(t) = \Delta E \sin(\omega t)$ . Where  $\Delta E$  was the signal amplitude (V).

$\omega$  was the pulse ( $\text{rad}\cdot\text{s}^{-1}$ ):  $\omega = 2\pi f$ .

Where  $f$  is the disturbance frequency in hertz ( $\text{s}^{-1}$ ).

Two graphical representations of the Z-transfer function ( $2\pi f$ ) are commonly used (1) in Cartesian coordinates, representing the imaginary part  $-\text{Im} Z(2\pi f)$  at the end of the real part of the transfer function  $\text{Re} Z(2\pi f)$ . This is the representation in the Nyquist plane and (2) in the Bode plane, denotes the logarithm of the modulus of the transfer function  $\ln |Z(2\pi f)|$  as well as the phase  $\varphi$  in the function of the logarithm of the frequency  $\ln(f)$ . For Impedance experiments, the same solutions (without/with LEO) of the chronoamperometric analysis were used; the experiments were carried out at a temperature of 40 °C under electroplating with a potential of  $-0.09$  V for 15 min for each test, using the same substrates of the presiding experiments. The variation of impedance was followed as a function of frequency. To test the reliability and reproducibility of the measurements, triplicate experiments were performed in each case at the same conditions.

## 3 Results and Discussion

### 3.1 Determination of LEO Yield and Density

*Lycium* leaves extracts comported about 18% of LEO with a density of 1.07 g/mL. These LEO contents varied depending on several factors such as climate, geographical area of collection, time of collection, and extraction method [11, 26, 27]. EO were obtained from plant material by several extraction methods, such as hydrodistillation [28, 29], organic solvent extraction [30, 31], microwave extraction [32], ultrasonic extraction [33] and pressing [34]. Plant extracts, such as EO, were employed as inhibitors in order to develop new cleaning chemicals for a green environment [11].

### 3.2 Effect of LEO on Nanoparticle-Doped UFM's Conductivity

The contact angle of the nanoparticle-doped UFM was analyzed. Generally, the membrane was hydrophilic when it had an affinity for water. In this case, a drop of water deposited on this membrane tended to spread out, thus reducing the contact angle. On the other hand, a hydrophobic membrane

**Table 3** Characteristics of the electrolyte solution

Parameters	Prepared solution
pH	8.1
DO (mg/L)	5.5
Conductivity (ms)	44.3
Salinity (ppt)	29.6

forms a high contact angle with the drop of water deposited on its surface. High hydrophobicity was characterized with high contact angle (Fig. 4).

We synthesized a hydrophobic UF membrane because the surface forms a very high contact angle of  $94.15^\circ$  that is greater than  $90^\circ$ . The major limitation of the UFM technique is mainly caused by the blockage of membrane pores. Therefore, the enhanced hydrophilicity of membranes is the key parameter to improve the performance of UFM [35]. UFM performance includes the (i) composition of the membrane related to the blend-ratio of several additives (namely, polymeric, inorganic, grafted polymers, etc.); (ii) operating conditions (pH, temperature, salinity, oil concentration, and cross-flow velocity of feed, the viscosity of casting solution and salinity of the coagulation bath, etc.); and (iii) process optimization [36]. The present work further provides insights into the fouling of membranes using nanoparticle-doped UFM. It emphasizes the challenges faced for applications of nanoparticle-doped UFM. Results presented in Table 4 showed that the solution's conductivity before filtration was about 97 ms/cm, which explains the existence of all mineral salts dissolved in  $\text{CaCl}_2$  solution. After the first frontal filtration of 50 mL solution of  $\text{CaCl}_2$  with nanoparticle-doped UFM, we obtained 15 mL of permeate and then filtration stopped. The conductivity of obtained permeate was about 46 ms/cm. These results showed that the mineral salts precipitated on the membrane and subsequently, pores of the membrane, were blocked by scale deposit.

For second frontal filtration following application of LEO on nanoparticle-doped UFM, we recovered 20 mL of permeate with very low conductivity equal to 1.13  $\mu\text{s}/\text{cm}$ , which indicated that precipitation did not occur and that LEO prevented dissolved ions from precipitating into calcium carbonate. We investigated whether LEO can be considered a novel environmentally friendly anti-scalant for  $\text{CaCO}_3$  calcareous deposits on steel in an alkaline  $\text{CaCl}_2$  brine solution. Previously, calcium carbonate precipitation after the addition of sodium carbonate was analyzed using the conductivity measurement test [11, 37]. As evidenced, the

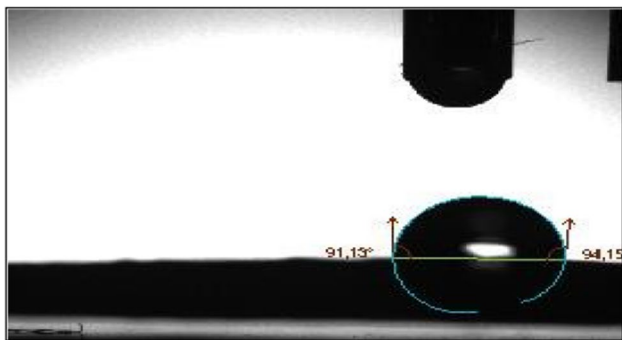


Fig. 4 Contact angle of UF membrane doped nanoparticles

**Table 4** Variation of permeability and conductivity of  $\text{CaCl}_2$  solution after filtration with MUF in the presence and absence of LEO at  $25^\circ\text{C}$

$\text{CaCl}_2$ Solution	Conductivity	Volume of permeate
Initial $\text{CaCl}_2$ Solution	97 ms/cm	–
Permeate 1 ( $\text{CaCl}_2$ Solution without LEO)	46 ms/cm	15 mL
Permeate 2 ( $\text{CaCl}_2$ Solution with LEO)	1.13 $\mu\text{s}/\text{cm}$	20 mL

conductivity of the solution reduced after the added amount of LEO and volume of permeate increased; the anti-scaling property was attributed to the presence of chelating agents of LEO [38]. We measured the ability of inhibitors to prevent the precipitation of calcium carbonate on nanoparticle-doped UFM. As previously suggested [11], the conductivity method elucidates the tendency of the extract to inhibit the scale in the solution, but also after frontal filtration on nanoparticle-doped UFM.

### 3.3 Study of Scaling Phenomenon by Electrochemical Process

Figure 5 shows the chronoamperometry curve for polarized steel electrodes in the  $\text{CaCl}_2$  brine solution in the absence and presence of LEO. After chronoamperometric analysis of the solution of  $\text{CaCl}_2$ ,  $\text{NaCl}$ ,  $\text{Na}_2\text{SO}_4$ ,  $\text{NaHCO}_3$ , the same solutions with LEO were determined. These analyses occurred 2 h under stirring, at  $40^\circ\text{C}$ , and at  $-0.9\text{ V}$ .

Without LEO, a high current variation with time exceeds  $-5.10^{-4}\text{ A}$  for 6000 S was observed. These results explained the strong charge transfer between the electrode

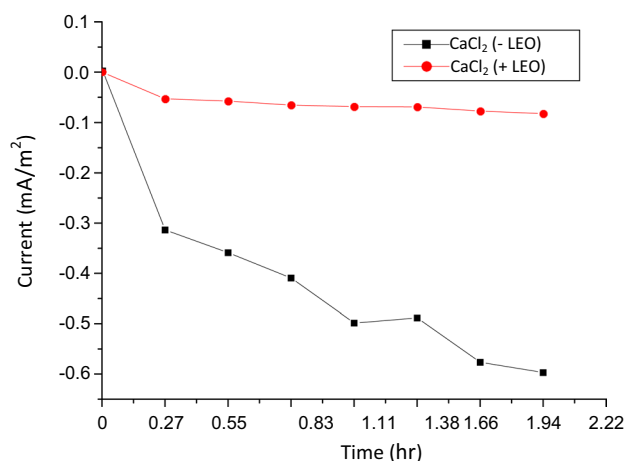


Fig. 5 Chronoamperometry curves for polarized steel electrode at  $-0.9\text{ V}$  (vs. SCE) in the  $\text{CaCl}_2$  brine solution in the absence (–) and the presence (+) of LEO at  $40^\circ\text{C}$



and the solution verified by the integration of the current

$$I : Q = -B \int A I . dt$$

$$Q = - [(-5.10^{-4}) - (-3.10^{-4})]$$

$$Q = -2.10^{-4} A.s$$

With LEO, a small variation of the current as a function of time remained almost constant at  $-5 \cdot 10^{-5}$  A for 2 h. This implies that the charge transfer between solutions and the conductive surface of the substrate decreased. The integration of  $I=f(t)$  gives a charge quantity  $Q = -4.10^{-5}$  A.s (Fig. 5). According to these findings, there was a complexation of  $Ca^{2+}$  by LEO probably due to the inhibitory action of LEO on the rate of reduction in oxygen where oxidation was zero. The amount of charge tolled proves the existence of free calcium and carbonate ions in the solution. The control test without LEO proved deposit of  $CaCO_3$  covered the conductive surface of the substrate at the end of the experiment (Fig. 6a). Test in the presence of LEO showed substrate without  $CaCO_3$  deposition (Fig. 6b).

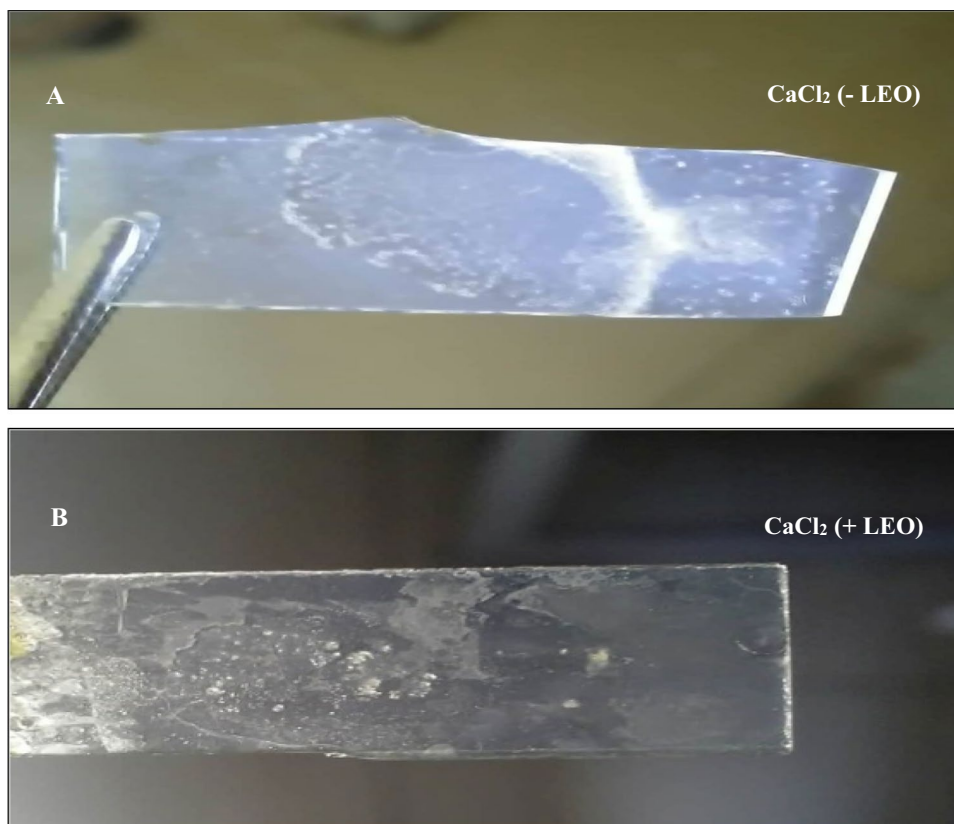
Scaling processes analyzed by the chronoamperometry technique have been documented by several investigators [39–42]. The current passing through the electrode is recorded with respect to time, while the electrode is polarized at the diffusion limiting current of oxygen. The scales

formed on metal surfaces under cathodic polarization, cover the active surface area available for the electrochemical reactions and consequently, reduce the current density [11, 43]. As seen in Fig. 5, the chronoamperometry curve for the polarized steel electrode in the  $CaCl_2$  brine solution at  $40^\circ C$  can be separated into three regions. The same plot was previously observed by Abdel-Gaber et al. [11] for chronoamperometry curves of cathodically polarized steel electrode at  $-0.9$  V in the  $CaCl_2$  brine solution in the absence and the presence of different concentrations of *Punica granatum* hull extract at  $40^\circ C$ . The authors attributed the initial current decrease to some decline in the oxygen reduction rate, strongly dependent on the electrode pretreatment, and the scaling process initialized by increasing the local pH near the electrode surface by utilizing the reduction in the dissolved oxygen in the brine solution. On the contrary, in presence of a low concentration of the *Punica granatum* extract (5 ppm), a total blocking of the electrode surface stage was not observed.

### 3.4 Impedance Study

The impedance technique's usage improved understanding of the electrochemical scaling process [11, 42, 44]. During the tests, an amplitude of  $-0.09$  V was adopted for the linearity of response between intensity and potential.

**Fig. 6** Substrate scaled by electrolyte solution in the absence (–) and the presence (+) of LEO



Frequencies of measurements were in (HZ). Impedance results were obtained in the form of graphs: Nyquist and bode. Without LEO, we noticed that loop diameter increased with the cathodic potential. Resistance  $R_p$  decreased with the potential improved development of deposits on the conductive surface of the substrate. In presence of LEO, we noticed a decrease in loop diameter with the cathodic potential, which led to an increase in polarization resistance probably due to adsorption of LEO on active sites of limestone deposits (Fig. 7).

The impedance spectra were used to characterize different scaling regions [11]. LEO impedes the rate of scale formation by bonding the chemical constituent to the cations present in the brine solution forming a soluble complex, or by dispersion of the suspended solids through adsorption [45]. According to the diagram of phase angle versus frequency (Fig. 8), we showed that the phase curve without LEO was attributed to the deposition of a layer formed on the electrode. By contrast, the second phase with LEO was related to the transfer charge through the deposition layer. Notably, the presence of LEO caused the shift of phase angle  $\Theta$  in the function of frequency. In literature, the higher frequency phase angle peak is most likely attributed to the formation of surface film because its appearance correlates with the surface dielectric film that normally has a small-time constant. Thus, it has a phase shift in the high-frequency range [11; 46, 47]. Results of electrochemical impedance spectroscopic EIS analysis proved that LEO played the role of

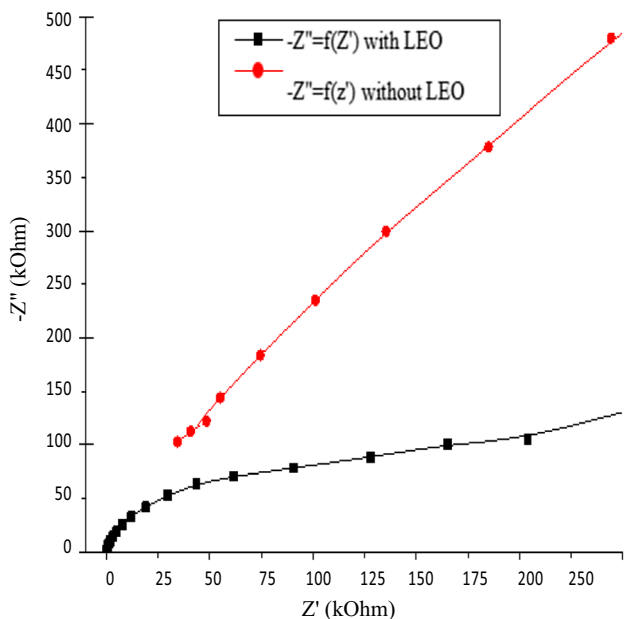


Fig. 7 Nyquist diagram obtained from the electroplating of the substrates used in chronoamperometry under an amplitude of  $-0.09$  V for 15 min

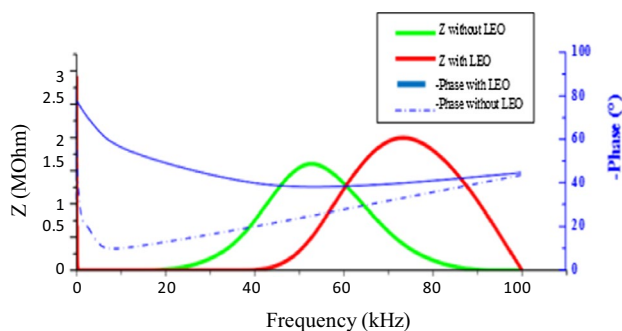


Fig. 8 Bode diagram obtained from the electroplating of the substrates used in chronoamperometry under an amplitude of  $-0.09$  V for 15 min

bio-flocculant, confirming the result obtained from chronoamperometry measurements.

### 4 Conclusion

Among the wild species and little studied, the *Lycium* plant was well valued and exploited in the pharmaceutical, industrial and cosmetic areas. We were first interested in the extraction and characterization of essential oils from leaves of *Lycium* harvested from shrubs growing in Borj Cedria, Tunisia. *Lycium* leaves comported about 18% of LEO with a density of 1.07 g/mL. To valorize LEO and resolve the problem of crystalline deposit formation in water circuits called the phenomenon of scaling, a membrane study was carried out by frontal filtration of  $CaCl_2$  solution through nanoparticle-doped UFM. The formation of scale deposits blocked membrane pores by precipitation of the dissolved salts on the membrane surface. The permeability decreased in the presence of  $CaCl_2$ , and we obtained a volume of 15 mL less than the initial volume (50 mL). After the spreading of the membrane by the LEO and the frontal filtration of the  $CaCl_2$  solution, we noticed that the volume of permeate increased (20 mL) and the conductivity decreased, thus improving the complexing of  $Ca^{2+}$  by the LEO. To evaluate the effect of LEO on the deposition of  $CaCl_2$ , we used the chronoamperometry technique to obtain fast scaling. Chronoamperometry curves were analyzed for cathodically polarized steel electrode at  $-0.9$  V in the  $CaCl_2$  brine solution in the absence and the presence of LEO at  $40$  °C. Without LEO, the polarization curve showed a very high current intensity, proving that the solution was very calcifying and contained many dissolved salts deposited in the interface of the substrate that caused an increase in charge transfer. A high current variation with time exceeding  $-5.10^{-4}$  A for 6000 s was observed. With LEO, a small variation of the current as a function of time remained almost constant at  $-5 \cdot 10^{-5}$  A for 2 h, which demonstrates that the charge transfer between solutions and

the conductive surface of the substrate decreased. The characterization of the deposits formed on the substrate after 15 min of electroplating by the electrochemical impedance spectroscopy EIS, allowed us to draw some parameters, namely the polarization resistance  $R_p$ . We noticed that the loop diameter increased with the cathodic potential. The polarization resistance,  $R_p$ , decreased with the potential improved development of deposits on the conductive surface of the substrate. The chronoamperometric analysis in the presence of LEO, which showed a drop in current and an increase in polarization resistance, proved that LEO was a good bio-flocculant and anti-scaling agent for membranes.

**Acknowledgements** The authors would like to thank all colleagues who have made this contribution possible. We are grateful to anonymous reviewers for helpful comments on the manuscript.

**Author Contributions** Zahrah Alhalili is responsible for doing the research practically, data collection and analysis. Hana Souli contributed to the design and implementation of research. Moêz Smiri provided the intellectual input and designed and approved the protocols to be followed in the study. He is responsible for the manuscript correction, proofreading, submission and revision.

**Funding** No funding was received.

## Declarations

**Conflict of interest** The authors declare that they have no conflict of interest.

**Data availability** All data generated or analyzed during this study are included in this published article.

## References

- Fukuda, T.; Yokoyama, J.; Ohashi, H.: Phylogeny and biogeography of the genus *Lycium* (Solanaceae): inferences from chloroplast DNA sequences. *Mol. Phylogenet. Evol.* **19**, 246–258 (2001)
- Boulila, A.; Mattosi, K.; Mrabet, Y.; Rokbeni, N.; Dhouioui, M.; Boussaid, M.: Determination of phytochemicals and antioxidant activity of methanol extracts obtained from the fruit and leaves of Tunisian *Lycium intricatum*. *Food chem.* **174**, 577–584 (2015)
- Master, M.: Study of a traditional plant from Tibet: the gogi, *lycium barbarum* (solanaceae). These of doctorate in pharmacy, University of Besançon, France (2011)
- Bonnier, G.: La grande flore en couleurs by Gaston Bonnier, Editions Belin, Paris, 355 pages (1990)
- Botineau, M. Botanique systématique et appliquée des plantes à fleurs, Editions Tech & Doc, Lavoisier 1336 pages (2010)
- Delaveau, P.: Expliquez-moi les plantes, voyage en botanique, Paris, Editions Pharmathèmes, 502 pages (2003)
- Hort, C.: Contribution to the study of scaling phenomena: influence of solids in contact with liquid on precipitation kinetics; PhD thesis INSA Toulouse, France (1994).
- Bessa, N.: Monograph of the valley of Oued R'hir. Recueil des communications des journées techniques et scientifiques sur la qualité des eaux du sud, page 5 (2003)
- Koribaa, B.: Prévention et lutte contre le phénomène d'entartrage dans les conduites d'eau dans la région de Ouargla-Touggourt. Thèse d'Université Kasdi Merbah Ouargla, Algeria (2007)
- Wang, C.C.; Chang, S.C.; Chen, B.H.: Chromatographic determination of polysaccharides in *Linnaeus*. *Chem.* **116**, 595–603 (2009)
- Abdel-Gaber, A.M.; Abd-El-Nabey, B.A.; Khamis, E.; Abd-El-Khalek, D.E.: Investigation of fig leaf extract as a novel environmentally friendly antiscalant for CaCO<sub>3</sub> calcareous deposits. *Desalin.* **230**, 314–328 (2008)
- Qiang, X.; Sheng, Z.; Zhang, H.: Study on scale inhibition performances and interaction mechanism of modified collagen. *Desalin.* **309**, 237–242 (2013)
- Kelland, M.A.: Effect of Various Cations on the Formation of Calcium Carbonate and Barium Sulfate Scale with and without Scale Inhibitors. *Ind. Eng. Chem. Res.* **50**, 5852–5861 (2011)
- Setta, F.A.; Neville, A.: Efficiency assessment of inhibitors on CaCO<sub>3</sub> precipitation kinetics in the bulk and deposition on a stainless-steel surface (316 L). *Desalin.* **281**, 340–347 (2011)
- Zhang, P.: Review of Synthesis and Evaluation of Inhibitor Nanomaterials for Oilfield Mineral Scale Control. *Front. Chem.* **19**, (2020)
- Guo, X.; Qiu, F.; Dong, K.; Rong, X.; He, K.; Xu, J.; Yang, D.: Preparation and application of copolymer modified with the palygorskite as inhibitor for calcium carbonate scale. *Appl. Clay Sci.* **99**, 187–193 (2014)
- Demadis, K.D.; Neofotistou, E.; Mavredaki, E.; Tsiknakis, M.; Sarigiannidou, E.M.; Katarachia, S.D.: Inorganic foulants in membrane systems: chemical control strategies and the contribution of “green chemistry.” *Desalin.* **179**, 281–295 (2005)
- Sharamon, S.; Baginski, B.J.: La baie de goji-un fruit hors du commun au pouvoir antioxydant surpuissant, p. 188p. Editions Médecis, Paris (2009)
- Amagase, H.; Farnsworth, N.R.: A review of botanical characteristics, phytochemistry, clinical relevance in efficacy and safety of fruit (Goji). *Lycium Barbarum*. *Food Res. Inter.* **44**, 1702–1717 (2011)
- PUNGIER, V.: Goji berries, Le Moniteur des pharmacies, n°2947, Cahier 1, **8**, (2012)
- Bakkali, F.; Averbeck, S.; Averbeck, D.; Idaomar, M.: Biological effects of essential oils - a review. *Food Chem. Toxicol.* **46**, 446–475 (2008)
- Tongnuanchan, P.; Benjakul, S.: Essential Oils: Extraction, Bio-activities, and Their Uses for Food Preservation. *J. Food Sci.* **79**, 1231–1249 (2014)
- Perineau, F.; Ganou, L.; Vilarem, G.: Studying production of lovage essential oils in a hydrodistillation pilot unit equipped with a cohobation system. *J. Chem. Tech. Biotech.* **53**, 165–171 (2007)
- Kumar, S.; Guria, C.; Mandal, A.: Synthesis, characterization and performance studies of polysulfone/bentonite nanoparticles mixed-matrix ultra-filtration membranes using oil field produced water. *Sep. Purif. Tech.* **150**, 145–158 (2015)
- Lédion, J.; Leroy, P.; Labbé, J.P.; Durand, G.; Leduigou, A.: L'entartrage par les eaux naturelles et l'action des appareils électriques antitartres. *Mat. Tech.* **68**(4–5), 139–144 (1980)
- Wang, L.; Weller, C.L.: Recent advances in extraction of nutraceuticals from plants. *Trends Food Sci. Technol.* **17**, 300–312 (2006)
- Starmans, D.A.J.; Nijhuis, H.H.: Extraction of secondary metabolites from plant material: A review. *Trends Food Sci. Tech.* **7**, 191–197 (1996)
- Meyer-Warnod, B.: Natural essential oils: extraction processes and application to some major oils. *Perfum. Flavorist* **9**, 93–104 (1984)
- Masango, P.: Cleaner production of essential oils by steam distillation. *J. Clean. Prod.* **13**, 833–839 (2005)

30. Faborode, M.O.; Favier, J.F.: Identification and significance of the oil-point in seed-oil expression. *J. Agric. Eng. Res.* **65**, 335–345 (1996)
31. Leybros, J.; Fremeaux P.: Solid-liquid extraction—Theoretical aspects, *Treatise Process Eng.*, J 2780 (1990)
32. Ericsson, M.; Colmsjö, A.: Dynamic microwave-assisted extraction. *J. Chrom. A* **877**, 141–151 (2000)
33. Kimbaris, A.C.; Siatis, N.G.; Daferera, D.J.; Tarantilis, P.A.; Pappas, C.S.; Polissiou, M.G.: Comparison of distillation and ultrasound-assisted extraction methods for the isolation of sensitive aroma compounds from garlic (*Allium sativum*). *Ultrasonics Sonochem.* **13**, 54–60 (2006)
34. Willem, J.P.: *Les Huiles essentielles : Médecine d'avenir*. Ed: Estem, Paris, 311 pages (2004)
35. Ahmad, T.; Guria, C.; Mandal, A.: A review of oily wastewater treatment using ultrafiltration membrane: A parametric study to enhance the membrane performance. *J. Water Proc. Eng.* **36**, 101289 (2020)
36. Gohari, J.R.; Halakoo, E.; Lau, W.J.; Kassim, M.A.; Matsuura, T.; Ismail, A.F.: Novel polyethersulfone (PES)/hydrous manganese dioxide (HMO) mixed matrix membranes with improved anti-fouling properties for oily wastewater treatment process. *RSC Adv.* **4**, 17587–17596 (2014)
37. Drela, I.; Falewicz, P.; Kuczkowska, S.: New rapid test for evaluation of scale inhibitors. *Water Res.* **32**, 3188–3191 (1998)
38. Wang, H.F.; Yih, K.H.; Yang, C.H.; Huang, K.F.: Anti-oxidant activity and major chemical component analyses of twenty-six commercially available essential oils. *J. Food Drug Anal.* **25**, 881–889 (2017)
39. Leroy, P.; Lin, W.; Ledion, J.; Khalil, A.: Caractérisation du pouvoir entartrant des eaux à l'aide d'essais d'électrodéposition; étude comparative de plusieurs méthodes. *J. Water SRT-Aqua* **42**, 1 (1993)
40. Deslouis, C.; Gabrielli, C.; Keddam, M.; Khalil, A.; Rosset, R.; Tribollet, B.; Zidoune, M.: Impedance techniques at partially blocked electrodes by scale deposition. *Electrochim. Acta* **42**, 1219–1233 (1997)
41. Deslouis, C.; Festy, D.; Gil, O.; Maillot, V.; Touzain, S.; Tribollet, B.: Characterization of calcareous deposits in artificial sea water by impedances techniques: 2-deposit of  $Mg(OH)_2$  without  $CaCO_3$ . *Electrochim. Acta* **45**, 1837–1845 (2000)
42. Gabrielli, C.; Keddam, M.; Khalil, A.; Rosset, R.; Zidoune, M.: Study of calcium carbonate scales by electrochemical impedance spectroscopy. *Electrochim. Acta* **42**, 1207–1218 (1997)
43. Yan, J.F.: Parametric Studies of the Formation of Calcareous Deposits on Cathodically Protected Steel in Seawater. *J. Electrochem. Soc.* **140**, 1275 (1993)
44. Sfaira, M.; Srhiri, A.; Takenouti, H.; Ficquelmont-Loïzos, M.M.; Bachir, A.B.; Khalakhil, M.: *J. Appl. Electrochem.* **31**, 537–546 (2001)
45. Bessone, J.B.; Salinas, D.R.; Mayer, C.E.; Ebert, M.; Lorenz, W.J.: An EIS study of aluminium barrier-type oxide films formed in different media. *Electrochim. Acta* **37**, 2283–2290 (1992)
46. Feliu, S.; Galván, J.C.; Feliu, S.; Bastidas, J.M.; Simancas, J.; Morcillo, M.; Almeida, E.M.: An electrochemical impedance study of the behaviour of some pretreatments applied to rusted steel surfaces. *Corrosion Sci.* **35**, 1351–1358 (1993)
47. Tsai, C.H.; Mansfeld, F.: Determination of coating deterioration with EIS: Part II development of a method for field testing of protective coatings. *Corros.* **49**(9), 726–737 (1993)

